High-Temperature Atomic Diffusion and Specific Heat in Quasicrystals

Yuki Nagai[1,2,3,*] Yutaka Iwasaki,[4,5,†] Koichi Kitahara,[6] Yoshiki Takagiwa,[4] Kaoru Kimura,[4,5] and Motoyuki Shiga[2]

[1]*Information Technology Center, The University of Tokyo, 6-2-3 Kashiwanoha, Kashiwa, Chiba 277-0882, Japan*
[2]*CCSE, Japan Atomic Energy Agency, 178-4-4 Wakashiba, Kashiwa, Chiba 277-0871, Japan*
[3]*Mathematical Science Team, RIKEN Center for Advanced Intelligence Project (AIP),*
1-4-1 Nihonbashi, Chuo-ku, Tokyo 103-0027, Japan
[4]*National Institute for Materials Science (NIMS), 1-2-1 Sengen, Tsukuba, Ibaraki 305-0047, Japan*
[5]*Department of Advanced Materials Science, The University of Tokyo, 5-1-5 Kashiwanoha, Kashiwa, Chiba 277-8561, Japan*
[6]*Department of Materials Science and Engineering, National Defense Academy,*
1-10-20 Hashirimizu, Yokosuka, 239-8686 Kanagawa, Japan

A quasicrystal is an ordered but nonperiodic structure understood as a projection from a higher-dimensional periodic structure. Some physical properties of quasicrystals are different from those of conventional solids. An anomalous increase in heat capacity at high temperatures has been discussed for over two decades as a manifestation of a hidden high dimensionality of quasicrystals. A plausible candidate for this origin has been the phason, which has excitation modes originating from the additional atomic rearrangements introduced by the quasiperiodic order, which can be understood in terms of shifting a higher-dimensional lattice. However, most theoretical studies of phasons have used toy models. A theoretical study of the heat capacity of realistic quasicrystals or their approximants has yet to be conducted because of the huge computational complexity. To bridge this gap between experiment and theory, we show experiments and molecular simulations on the same material, an Al-Pd-Ru quasicrystal, and its approximants. We show that at high temperatures, aluminum atoms diffuse with discontinuouslike jumps, and the diffusion paths of the aluminum can be understood in terms of jumps corresponding to hyperatomic-fluctuations-associated atomic rearrangements of the phason degrees of freedom. It is concluded that the anomaly in the heat capacity of quasicrystals arises from the hyperatomic fluctuations that play a role in diffusive Nambu-Goldstone modes.

Introduction.—Quasicrystals (QCs) [1,2] are solids with quasiperiodic atomic structures. Mathematically, a quasi-periodic structure is constructed by a projection from a higher-dimensional space [3]: Every quasiperiodic structure in three-dimensional physical space can be described as a projection from a hypothetical higher-dimensional periodic crystal structure called a "hyperlattice." The hyperlattice concept is commonly used to explain the static structures of QCs [4,5].

QCs have unique physical properties that are not observed in conventional solids [6–8]. In particular, several quasicrystals at high temperatures show significant increases in heat capacity. The heat capacity per atom at a constant volume c_V for icosahedral Al-Pd-Mn [9–11], Al-Cu-Fe [12], Al-Cu-Ru [13], and decagonal Al-Cu-Co [9,10] QCs show large upward deviations from the Dulong-Petit limit $3k_B$, where k_B is the Boltzmann constant. Such anomalous heat capacity at high temperatures has been debated for over two decades, and a potential connection with the hidden higher-dimensional properties of QCs has been discussed.

The phason [11,14,15], has been suggested as the origin of the high-temperature anomalous heat capacity [11,16]. The phason modes originate from the fact that the free energy of the system is invariant under a rigid translation of the parallel space in the perpendicular dimension, where the hyperlattice decomposes into the parallel (physical) and the perpendicular space. In many solids, heat capacity at high temperatures approaches the Dulong-Petit limit $3k_B$, because full vibrational-mode degrees of freedom amount to 3 degrees of freedom per atom, each corresponding to a quadratic kinetic energy term and a harmonic potential energy term. However, the vibrations in QCs are beyond harmonic oscillations along the phason degrees of freedom, which may contribute to the increased heat capacity. Inelastic neutron scattering [17] and coherent x-ray scattering [18] experiments on Al-Pd-Mn QC have observed characteristic phason excitation and diffusive modes above approximately 700 K. These results suggest that the phason is excited at high temperatures with anomalous atomic motion, consistent with the temperature range where anomalous heat capacity is observed. In addition, experimental evidence of anomalous atomic vibrations at specific atomic sites in the structure at 1100 K has been observed in decagonal Al-Ni-Co QCs [19].

Further evidence that the phason may be the cause of the anomalous heat capacity is seen in the relationship between the degree of approximation and the heat capacity in quasicrystalline approximant crystals (ACs), which are periodic crystals that have the same local structure as the corresponding QC. The structure of ACs is classified by the degree of approximation represented by two consecutive numbers in the Fibonacci sequence, such as $1/0, 1/1, 2/1, \ldots,$ q_n/q_{n-1}. A larger q_n in an AC corresponds to a larger unit cell and a structure that is closer to that of a QC. As the degree of approximation increases, the AC becomes closer in structure to the QC. The AC-specific heat is expected to become more anomalous as it approaches the QC limit because the phason degrees of freedom may increase [11,13].

So far, most theoretical studies of phasons have used toy models consisting of a single atomic species in one or two dimensions [20,21]. The three-dimensional atomic motion of multiple-element QCs has been studied experimentally in decagonal phases such as Al-Ni-Co QCs [19]. In a recent molecular dynamics (MD) simulation by Mihalkovič and Widom [22], an AC of Al-Cu-Fe quasicrystals containing 9846 atoms was studied, focusing on its energetic stability. However, it is not clear what contributes to the high-temperature anomalous heat capacity in actual materials, although the phason is a plausible candidate. Additionally, a direct computation of heat capacity has never been done before because adequately describing the dynamic behavior of QCs accounting for a huge number of atoms and complex atomic interactions is required.

To bridge this large gap between experiment and theory, we study the same material from both theoretical and experimental approaches. First, we synthesized Al-Pd-Ru icosahedral QC and its ACs and observed the high-temperature anomalous heat capacity. We then performed a machine-learning molecular dynamics (MLMD) simulation for Al-Pd-Ru ACs and qualitatively reproduced the increase of the heat capacity. We herein show that Al atoms diffuse with discontinuous jumps at the temperature range where anomalous heat capacity is observed. The diffusion path of Al atoms can be understood in terms of hyperatomic fluctuations in six-dimensional space—associated atomic rearrangements in three-dimensional space. Considering this atomic diffusion due to hyperatomic fluctuations to be the "phason" diffusion, this diffusion can be understood as a diffusive Nambu-Goldsone mode. Based on this observation, we conclude that atomic diffusion due to hyperatomic fluctuations in hyperdimensional space, which consists of a series of discontinuous atomic jumps, is the origin of the high-temperature anomalous heat capacity.

Heat capacity: Experiment and simulation.—Figure 1(a) shows the experimental results of the constant-volume heat capacity C_V of Al-Pd-Ru icosahedral QC and its ACs. It can be seen that C_V largely deviates from Dulon-Petit's law, $3k_B$ with increasing temperature. The deviation from the $3k_B$ is the largest for QCs, followed by the 2/1 AC and 1/0 AC. Thus, the C_V anomaly of the ACs increases as the AC structure becomes similar to the QC. This systematical trend is consistent with previous work [11] that reported C_V values for various aluminum-transition-metal QCs and ACs.

The MLMD simulations of Al-Pd-Ru ACs are conducted under periodic boundary conditions. We used a potential energy function from an artificial neural network (ANN) that imitates the Born-Oppenheimer energies obtained by first-principles density-functional theory. The ANN was trained by a self-learning hybrid Monte Carlo method [23,24] with a combination of PIMD [23,25], the Vienna Ab initio Simulation Package [26,27], and Atomic Energy Network [28] software. The computational details are provided in the Supplemental Material [29].

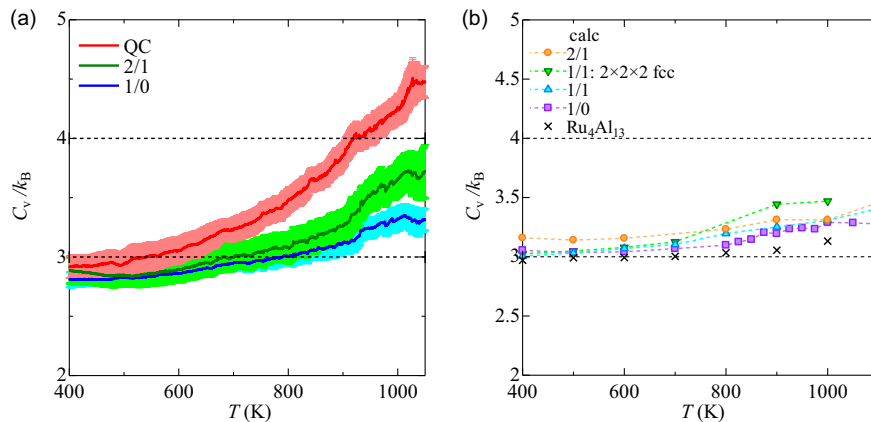We show the heat capacity directly calculated by the ensemble average of the energy fluctuation as

FIG. 1. Temperature dependence of heat capacity at constant volume normalized by Boltzmann constant C_V/k_B (a) in the experiment for Al-Pd-Ru QC (red), 2/1 AC (green), and 1/0 AC (blue), and (b) in the calculation for 2/1 AC (orange circle), 1/1 AC (blue triangle), 1/1 AC with $2 \times 2 \times 2$ face-centered-cubic primitive supercell (green triangle), 1/0 AC (purple square), and Ru_4Al_{13} (cross), where the thick light-colored line on each measured line stands for the standard deviation.

$C_V = \langle (\Delta E)^2 \rangle / (k_B T^2)$. Figure 1(b) shows the calculated heat capacity for $Al_{13}Ru_4$, 1/0, 1/1, and 2/1 Al-Pd-Ru ACs. The simulation of $Al_{13}Ru_4$ reproduces the conventional Dulong-Petit limit $3k_B$ as observed in experiments [13]. For ACs, we found that the calculated heat capacity depends on the temperature and becomes larger than the Dulong-Petit limit at high temperature. Here, the difference between 1/1 AC and 1/1 AC with $2 \times 2 \times 2$ face-centered-cubic primitive cells in Fig. 1(b) is the difference of the number of atoms in a unit cell, 128 and 256, respectively. There is some system size dependence in the simulated results for the 1/1 AC case. To make a qualitative comparison with experiment, one needs to add more atoms in the unit cell, although such a computation is too expensive at present.

Atomic structure and phasons.—The local atomic structures of the QCs and ACs are similar, the main difference being how the cluster structures are connected. Therefore, the cause of the anomalous heat capacity in QCs can be revealed by calculating the corresponding ACs. To understand high-temperature anomalous heat capacity, we introduce the crystal structure of ACs in the Al-Pd-Ru system.

Figure 2 shows the 1/0 AC, 1/1 AC, and 2/1 AC model structures generated by the modified Katz-Gratias-Boudard model of the Al-Pd-Ru system [30–32]. The structure of Al-Pd-Ru ACs is described as a dense packing of two types of clusters [33], the so-called mini-Bergman and pseudo-Mackay clusters shown in Figs. 2(d) and 2(e), respectively. These structures were obtained assuming the smallest size of the hyperatoms in six dimensions called "the occupation domain." Note, however, that these model structures are not necessarily energetically favorable and may not represent the actual structure of the AC at finite temperatures. The actual structural ensemble in thermal equilibrium can only be obtained after MD simulations. In the next section, we will show the results of the MD simulations starting from these model structures.

MD analysis.—MD simulations of Al-Pd-Ru AC show several energetically favorable structures apart from the prototype shown in Fig. 2. Those structures are different at the Al sites. It was found that some Al atoms are mobile in the ACs and randomly jump from one site to another during MD simulations in thermal equilibrium. This jump is detected at high temperatures where the heat capacity becomes anomalous.

Figures 3(a)–3(c) show the trajectories of some Al atoms for 1/1 AC at a temperature of 1000 K. Pd, Ru, and some Al atoms composing the inner shell of the mini-Bergman cluster are immobile and oscillate at their respective positions, as shown in Fig. 3(a). However, some other Al atoms composing the inner shell and edge of the pseudo-Mackay cluster are moving with almost discontinuous jumps, as shown in Figs. 3(b) and 3(c). This may correspond to what was predicted as "phason flips" in the QC model system [21,34], but detecting atomic jumps in real time from MD simulations is a new finding. At 1000 K, the atomic jumps occur at about 100 ps, which is much longer than conventional phonon oscillations; an analysis of trajectories up to 2 ns suggests that the moving Al atoms diffuse across the AC, as shown in the next subsection.
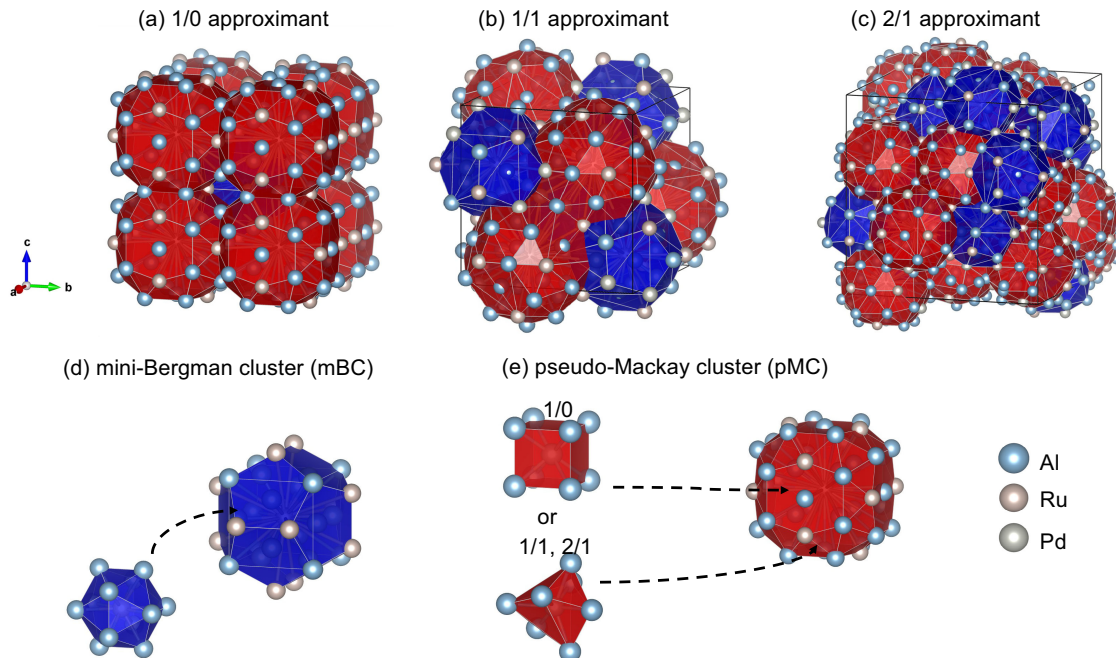

FIG. 2. Atomic structures of Al-Pd-Ru ACs: (a) 1/0 AC, (b) 1/1 AC, (c) 2/1 AC, (d) Mini-Bergman cluster, and (e) The pseudo-Mackay cluster of each AC. Here, the mini-Bergman and pseudo-Mackay clusters have an inner shell.
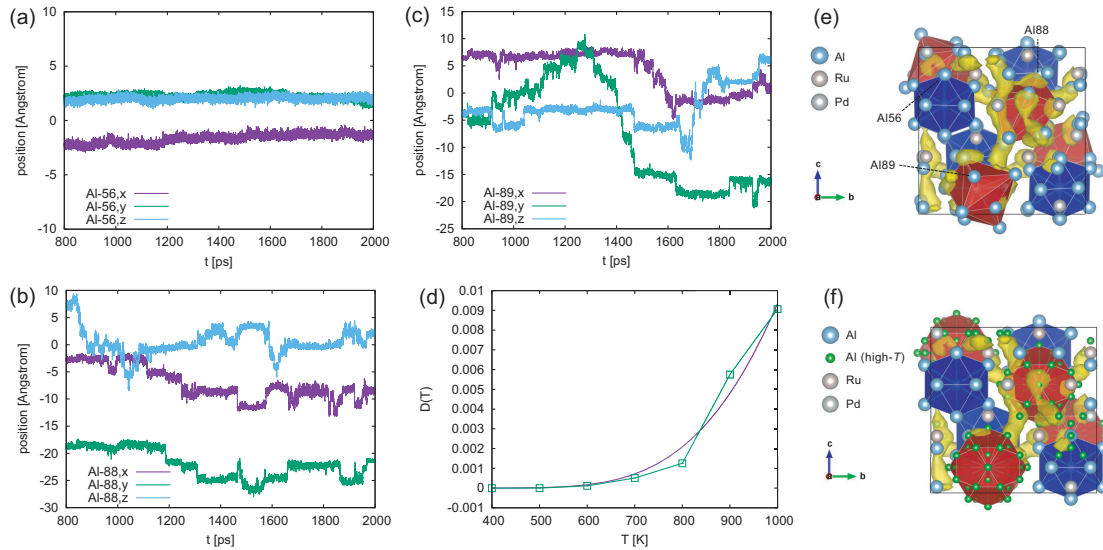
FIG. 3.   (a)–(c) Real-time dynamics of the Al atoms in the 1/1 AC $Al_{92}Pd_{20}Ru_{16}$ at 1000 K. (d) Temperature dependence of the diffusion coefficient. Visualization of the diffusive Al atoms in (e) the initial atomic structure and (f) atoms generated by the hyperatom in the six-dimensional space. Here, the yellow isosurface and the blue and red polyhedra represent the three-dimensional distribution of the Al atoms for 1/1 AC at $T = 1000$ K from $t = 800$ to 2000 ps, and the inner shell of the mini-Bergman and pseudo-Mackay clusters, respectively.

Figure 3(d) shows the diffusion coefficients $D(T)$ of the Al atoms in 1/1 AC, which are obtained from the slope of the mean square displacement of the moving Al atoms; see Supplemental Material [29] for the computational details. By a linear fitting of the Arrhenius plot of $D(T)$, the free-energy barrier of the Al jumps is estimated as $\Delta E \sim 6000$ K ($\sim$0.52 eV), which is reachable at the high-temperature range exhibiting the anomalous heat capacity. Here it is worth noting that the diffusion of Al atoms in ACs (and presumably in QCs) occurs without any vacancy formation, as opposed to most diffusion mechanisms in perfect crystals. Figure 3(e) visualizes the trajectory of the Al diffusion. One can see that the diffusive paths are restricted within the locations at the edge of the mini-Bergman and pseudo-Mackay clusters shown in Fig. 2.

Discussion.—How can we understand the diffusion pathways? As mentioned earlier, the static configurations of the QCs and ACs correspond to the projection of hyperatoms on a periodic lattice in a higher-dimensional space. Figures 4(a) and 4(b) show the positions of the hyperatomic sites and atoms in the real space of the Al-Pd-Ru icosahedrons QC and AC, respectively. Here, the hyperatomic sites of the Pd and Ru atoms are located inside the hyperatomic shell, while the Al atoms are located outside. The hyperatomic sites shown in Fig. 4(a) are schematic. In this case, the QC and AC static configurations correspond to the most compactly occupied hyperatomic sites in six-dimensional space. However, there are many other accessible hyperatomic Al sites outside the shell. The accessibility of each of these sites is energy dependent and can only be determined after MD simulations. The

movement between the different hyperatomic sites corresponds to a phason flip, and a series of phason flips were observed at finite temperatures in the MD simulations. At higher temperatures, the occupancy of Al hyperatomic sites beyond the outer shell increases, resulting in the Al coordination shown in Fig. 4(b). This corresponds exactly to the diffusion path of Al atoms as found in the MD simulation shown in Fig. 3(f). Therefore, the Al diffusion in the Al-Pd-Ru QC and AC can be regarded as a six-dimensional hyperatomic fluctuation.
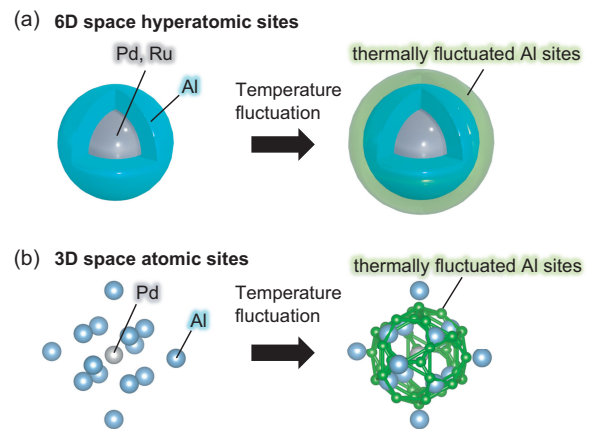

FIG. 4.   (a) Schematic figure of the effect of temperature fluctuation of the hyperatom in six-dimensional space. Al atoms are located around the surface. (b) Schematic figure of the effect of a temperature fluctuation of the corresponding atoms composing the inner shell of the pseudo-Mackay cluster in three-dimensional space.

Why does the heat capacity become anomalous in the presence of phason flips? The heat capacity follows the Dulong-Petit rule assuming harmonic vibrations of conventional phonons. The anomaly thus arises from the anharmonicity of the potential energy surface with respect to the phason flips involving Al jumps. In fact, heat capacity generally exhibits a complex temperature dependence in the presence of anharmonic or diffusive degrees of freedom [35]. According to QC hydrodynamics, phason flips correspond to diffusive Nambu-Goldstone modes [16,36]. Their dispersion relation is expressed as

$$\omega = -iD(T)q^2 + \cdots, \tag{1}$$

where q denotes the momentum of the phason mode. The analysis of Nambu-Goldstone modes is valid in ACs since near-degenerated states in ACs can be regarded as degenerated states in high temperatures. In this case, the imaginary frequency of the diffusive mode $i\omega$ is proportional to the diffusion coefficient $D(T)$. The magnitude of the heat capacity is determined by how much energy a material absorbs when heat is applied from the outside. Because the applied heat is partially used to excite the diffusive Nambu-Goldstone mode, the heat capacity becomes larger with increasing temperature.

Fully comprehending the dependence of specific heat on the p/q ratio in ACs remains an open question for future research. While our simulations did not reveal confined atomic motions within clusters, such movements could potentially contribute to the observed specific heat variations across ACs with different p/q ratios. This possibility warrants further investigation.

Summary.—The anomalous heat capacity observed in icosahedral AC in the Al-Pd-Ru system was well reproduced by machine-learning MD simulations. Some of the Al atoms were found to diffuse through the crystal in the absence of vacancies via nearly discontinuous jumps that can be regarded as phason flips. The restricted pathways of the phason flips can be understood as thermal fluctuations of hyperatoms in six-dimensional space—associated atomic rearrangements in three-dimensional space. From this result, we concluded that anomalous heat capacity is caused by atomic diffusion due to thermal fluctuations of hyperatoms in the higher-dimensional space in QCs and ACs. This study suggests that the high dimensionality of the QC structure may affect physical properties other than heat capacity.

———————

*nagai.yuki@mail.u-tokyo.ac.jp
†IWASAKI.Yutaka@nims.go.jp

[1] D. Shechtman, I. Blech, D. Gratias, and J. W. Cahn, Metallic phase with long-range orientational order and no translational symmetry, Phys. Rev. Lett. **53**, 1951 (1984).

[2] D. Levine and P. J. Steinhardt, Quasicrystals: A new class of ordered structures, Phys. Rev. Lett. **53**, 2477 (1984).

[3] A. Yamamoto, Crystallography of quasiperiodic crystals, Acta Crystallogr. Sect. A **52**, 509 (1996).

[4] M. Boudard, M. de Boissieu, C. Janot, G. Heger, C. Beeli, H. U. Nissen, H. Vincent, R. Ibberson, M. Audier, and J. M. Dubois, Neutron and x-ray single-crystal study of the AlPdMn icosahedral phase, J. Phys. Condens. Matter **4**, 10149 (1992).

[5] H. Takakura, C. P. Gómez, A. Yamamoto, M. De Boissieu, and A. P. Tsai, Atomic structure of the binary icosahedral Yb–Cd quasicrystal, Nat. Mater. **6**, 58 (2007).

[6] K. Deguchi, S. Matsukawa, N. K. Sato, T. Hattori, K. Ishida, H. Takakura, and T. Ishimasa, Quantum critical state in a magnetic quasicrystal, Nat. Mater. **11**, 1013 (2012).

[7] K. Kamiya, T. Takeuchi, N. Kabeya, N. Wada, T. Ishimasa, A. Ochiai, K. Deguchi, K. Imura, and N. K. Sato, Discovery of superconductivity in quasicrystal, Nat. Commun. **9**, 154 (2018).

[8] R. Tamura, A. Ishikawa, S. Suzuki, T. Kotajima, Y. Tanaka, T. Seki, N. Shibata, T. Yamada, T. Fujii, C.-W. Wang, M. Avdeev, K. Nawa, D. Okuyama, and T. J. Sato, Experimental observation of long-range magnetic order in icosahedral quasicrystals, J. Am. Chem. Soc. **143**, 19938 (2021).

[9] K. Edagawa and K. Kajiyama, High temperature specific heat of Al–Pd–Mn and Al–Cu–Co quasicrystals, Mater. Sci. Eng. A **294–296**, 646 (2000).

[10] K. Edagawa, K. Kajiyama, R. Tamura, and S. Takeuchi, High-temperature specific heat of quasicrystals and a crystal approximant, Mater. Sci. Eng. A **312**, 293 (2001).

[11] K. Fukushima, H. Suyama, Y. Tokumoto, Y. Kamimura, Y. Takagiwa, and K. Edagawa, Comparative study of high-temperature specific heat for Al–Pd–Mn icosahedral quasicrystals and crystal approximants, J. Phys. Commun. **5**, 085002 (2021).

[12] A. F. Prekul, V. A. Kazantsev, N. I. Shchegolikhina, R. I. Gulyaeva, and K. Edagawa, High-temperature heat capacity of the $Al_{63}Cu_{25}Fe_{12}$ quasicrystal, Phys. Solid State **50**, 2013 (2008).

[13] S. Tamura, K. Fukushima, Y. Tokumoto, Y. Takagiwa, and K. Edagawa, High-temperature specific heat of Al–Cu–Ru icosahedral quasicrystals and 1/1 crystal approximants, Mater. Trans., JIM **62**, 356 (2021).

[14] D. Levine, T. C. Lubensky, S. Ostlund, S. Ramaswamy, P. J. Steinhardt, and J. Toner, Elasticity and dislocations in

pentagonal and icosahedral quasicrystals, Phys. Rev. Lett. **54,** 1520 (1985).

[15] J. E. S. Socolar, T. C. Lubensky, and P. J. Steinhardt, Phonons, phasons, and dislocations in quasicrystals, Phys. Rev. B **34,** 3345 (1986).

[16] M. Baggioli and M. Landry, Effective field theory for quasicrystals and phasons dynamics, SciPost Phys. **9,** 062 (2020).

[17] G. Coddens, S. Lyonnard, B. Hennion, and Y. Calvayrac, Triple-axis neutron-scattering study of phason dynamics in Al-Mn-Pd quasicrystals, Phys. Rev. B **62,** 6268 (2000).

[18] S. Francoual, F. Livet, M. de Boissieu, F. Yakhou, F. Bley, A. Létoublon, R. Caudron, and J. Gastaldi, Dynamics of phason fluctuations in the $i-$AlPdMn quasicrystal, Phys. Rev. Lett. **91,** 225501 (2003).

[19] E. Abe, S. J. Pennycook, and A. P. Tsai, Direct observation of a local thermal vibration anomaly in a quasicrystal, Nature (London) **421,** 347 (2003).

[20] M. Engel, S. Sonntag, H. Lipp, and H.-R. Trebin, Structure factors of harmonic and anharmonic fibonacci chains by molecular dynamics simulations, Phys. Rev. B **75,** 144203 (2007).

[21] M. Engel, M. Umezaki, H.-R. Trebin, and T. Odagaki, Dynamics of particle flips in two-dimensional quasicrystals, Phys. Rev. B **82,** 134206 (2010).

[22] M. Mihalkovič and M. Widom, Spontaneous formation of thermodynamically stable Al-Cu-Fe icosahedral quasicrystal from realistic atomistic simulations, Phys. Rev. Res. **2,** 013196 (2020).

[23] Y. Nagai, M. Okumura, K. Kobayashi, and M. Shiga, Self-learning hybrid Monte Carlo: A first-principles approach, Phys. Rev. B **102,** 041124(R) (2020).

[24] K. Kobayashi, Y. Nagai, M. Itakura, and M. Shiga, Self-learning hybrid Monte Carlo method for isothermal–isobaric ensemble: Application to liquid silica, J. Chem. Phys. **155,** 034106 (2021).

[25] M. Shiga, PIMD: An open-source software for parallel molecular simulations, https://ccse.jaea.go.jp/software/PIMD/index.en.html.

[26] G. Kresse and J. Hafner, *Ab initio* molecular dynamics for liquid metals, Phys. Rev. B **47,** 558 (1993).

[27] G. Kresse and J. Furthmüller, Efficient iterative schemes for *ab initio* total-energy calculations using a plane-wave basis set, Phys. Rev. B **54,** 11169 (1996).

[28] N. Artrith and A. Urban, An implementation of artificial neural-network potentials for atomistic materials simulations: Performance for TiO_2, Comput. Mater. Sci. **114,** 135 (2016).

[29] See Supplemental Material at http://link.aps.org/supplemental/10.1103/PhysRevLett.132.196301 for information about sample preparation, characterization, physical properties analysis in experiments and detailed information about simulations are provided.

[30] M. Krajčí, M. Windisch, J. Hafner, G. Kresse, and M. Mihalkovič, Atomic and electronic structure of icosahedral Al-Pd-Mn alloys and approximant phases, Phys. Rev. B **51,** 17355 (1995).

[31] M. Krajčí and J. Hafner, Semiconducting Al–transition-metal quasicrystals, Phys. Rev. B **68,** 165202 (2003).

[32] M. Krajčí and J. Hafner, Topologically induced semiconductivity in icosahedral Al-Pd-Re and its approximants, Phys. Rev. B **75,** 024116 (2007).

[33] N. Fujita, H. Takano, A. Yamamoto, and A.-P. Tsai, Cluster-packing geometry for Al-based *F*-type icosahedral alloys, Acta Crystallogr. Sect. A **69,** 322 (2013).

[34] M. Widom, Discussion of phasons in quasicrystals and their dynamics, Philos. Mag. **88,** 2339 (2008).

[35] R. B. McClurg, R. C. Flagan, and W. A. Goddard, The hindered rotor density-of-states interpolation function, J. Chem. Phys. **106,** 6675 (1997).

[36] M. Baggioli, Homogeneous holographic viscoelastic models and quasicrystals, Phys. Rev. Res. **2,** 022022(R) (2020).